Localized Measurements of Wake Density Fluctuations Using Pulsed Laser Holographic Interferometry

A. B. WITTE,* J. FOX,† AND H. RUNGALDIER‡
TRW Systems Group, Redondo Beach, Calif.

A new technique of measuring localized wake turbulent fluctuations using pulsed laser holographic interferometry in a ballistic range has produced new data in a region normally inaccessible to support-free magnetically suspended wind-tunnel model testing (restricted to $X/D \leq 10$) or ballistic range anemometer measurements (restricted to $X/D \geq 400$). Extensive data were obtained with $\frac{1}{2}$ in. diam spheres and preliminary data with 12.5° half-angle, $\frac{3}{8}$ in. base diam cones fired at about 6000 fps at 1 atm in TRW Ballistic Range A. Sphere wake fringe data were reduced to obtain power spectral density, autocorrelation, cross correlation, cross spectra, and integral scale of the turbulent fluctuations in density. The present integral-scale data for sphere wakes appear to be somewhat above the Lees-Hromas-Webb theory for $25 \leq X/D \leq 400$ but within the projected range of wake anemometer data.

Nomenclature

A = projected area
C_D = drag coefficient
D = body diameter
$E_{1\rho}(f)$ = one-dimensional energy spectrum
f = space frequency
M = Mach number
p = pressure
R = gas constant, body radius
T = temperature
U = wake centerline velocity
u = velocity in projectile fixed coordinates
Λ = density integral scale
ρ = density

Superscript
$( )'$ = rms quantity

Subscripts
∞ = projectile flow condition
b = body
t = total condition

Introduction

IN a previous paper, axisymmetric mean density fields were calculated from holographic interferograms taken of 22 caliber models fired at about 3000 fps and at 1 atm in a small ballistic range equipped with a 6-in. scene depth holocamera.[1]

The broad objective of this paper is to show that pulsed laser holographic interferometry is a valuable diagnostic tool to measure turbulent wake density fluctuations produced by high-speed models fired in a large ballistic range. Of particular emphasis here is the use of this technique to measure wake density fluctuations in regions normally excluded to anemometry in the ballistic range ($X/D \leq 400$) and to the magnetically supported models in a wind tunnel ($X/D \geq 10$). With this goal in mind, holographic interferograms were recorded of the wake produced by $\frac{1}{2}$-in.-diam spheres and 12.5° half-angle, $\frac{3}{8}$-in.-base-diam cones fired at about 6000 fps and at 1 atm in Ballistic Range A at TRW. In contrast to the work done by Lien,[2] this present paper provides sphere wake data closer to the body and emphasizes the cross-beam localization rather than single-beam integrated turbulent wake properties.

On the basis of former work,[3] it would appear that a holocamera having more than 90° continuous viewing angle (or about twice that of the present state-of-the-art) is required to extract general 3-D density field from holograms. However, it is believed that the local statistical properties of a turbulent wake can be extracted, if, say, two views are taken at rather large angular separation (say, 90°) and a cross view localization analysis is applied.[4] This concept of "localization" by cross-beam viewing differs from the standard method[5] in that phase rather than intensity of the beams is measured and correlated. The technique will be discussed later on in the section on Data Reduction Techniques.

In subsequent sections of this paper, turbulent fluctuation data are calculated from the integrated single-beam and cross-beam measurements, and comparisons are made between these data and Fox's anemometer data,[6] other sources of data, and the Lees-Hromas-Webb (LHW) theory for wakes.[7,8]

Experimental Set-Up

In the present work, a dual beam holocamera is used to record two holograms simultaneously in intersecting orthogonal views of TRW Ballistic Range A. The two beams span about two feet more than the 4-ft port-to-port distance across the Range. Because the hologram is recorded over a large scene depth, each view has a rather modest viewing angle of 6.5°; however, the 3-D character of the flow phenomena, particularly the wake, is very noticeable as one views the hologram from side to side. The 3-D properties of these holograms have been particularly helpful in interpreting the interferogram fringe pattern as well as providing additional data.

The laser pulse length is about 100 nsec and the energy released from the Q-switched solid-state ruby is about 1 joule. The total energy is sufficient to adequately expose both vertical and horizontal beam holograms which are recorded on Agfa-Gevaert 8E75 plates. Because the projectile moves only about 0.005 in. during its exposure, the phenomena are "frozen" in the hologram. Holographic interferometry is accomplished by two exposures of the holographic plate, one before and one during the test. Details of the holocamera and laser illuminator are presented in Ref. 1.

Discussion of Wake Holographic Interferograms

Infinite Fringe and Finite Fringe Interferograms

The holographic interferograms, shown below were recorded by either an infinite fringe or finite fringe technique. In the former technique none of the optics is moved between the individual recordings of the comparison scene and subject scene

Presented as Paper 70-727 at the AIAA Reacting Turbulent Flows Conference, San Diego, Calif., June 17–18, 1970; submitted September 24, 1970; revision received November 19, 1971. This research was sponsored by the ABMDA and monitored by the ABMDAH under Mod P001 to Contract DAHC 60-69-C-0006. The authors wish to thank W. H. Webb posthumously for his technical assistance and F. Gomes for his assistance in conducting the experiments.

Index categories: Jets, Wakes, and Viscid-Inviscid Flow Interaction; Lasers.

* Head, Experimental Staff, Fluid Mechanics Laboratory. Member AIAA.

† Staff Engineer, Reentry Physics Department. Member AIAA.

‡ Member of the Professional Staff, Engineering Technology Department. Member AIAA.

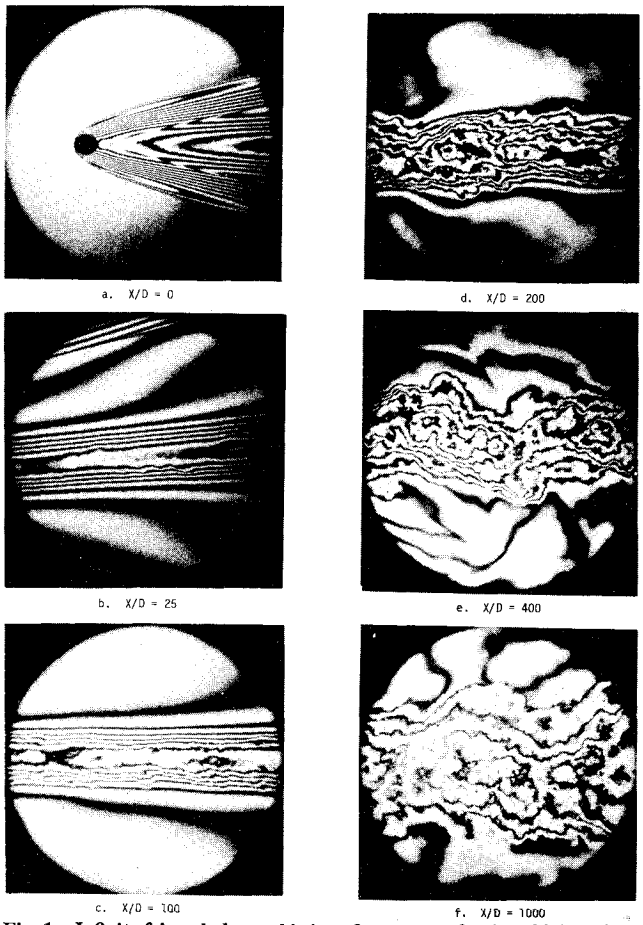

Fig. 1 Infinite fringe holographic interferograms of wake of $\frac{1}{2}$-in. sphere fired at 6000 fps, 1 atm.

in the common path interferometer. In the finite fringe technique the photographic plate is rotated between recordings so as to form a raster of interference fringes. Fringe shift is measured relative to the background parallel raster of fringes. The technique is quite analogous to that used in standard Mach-Zehnder interferometry.

The first step in the data reduction technique is to reconstruct the hologram with a cw laser and to photographically copy the data. The procedure is discussed elsewhere.[1]

Before density data can be computed from interferograms, fringe number or fringe shift and fringe position must be recorded from the interferogram. Fringe number is the number of wavelengths that the emitted light is advanced or retarded in phase as it proceeds through the disturbance. The infinite fringe interferogram produces fringes of constant phase. Without some a priori knowledge of the flowfield, like flow through a shock wave produces an increase in density, it may not be apparent what value a fringe assumes, i.e., an increase, decrease, or unchanged fringe number. Thus, an ambiguity in fringe number can occur. For the cases considered here, this can be a problem when measuring the turbulent fluctuations that exist along the wake centerline for $X/D \geqq 100$. Somewhat off the wake centerline and also in the remainder of the inviscid flowfield, fringe interpretation is straight forward.

The fringe ambiguity problem along the wake centerline was eliminated by recording finite fringe interferograms. Fringe shift for these interferograms in number of fringes or wavelengths, is measured from a reference raster or fringes located in an undisturbed part of the flowfield.

Sphere Wakes—Infinite Fringe Interferograms

A sequence of infinite fringe interferograms of the sphere wake for $0 \leqq X/D \leqq 1000$ is shown in Fig. 1. The $\frac{1}{2}$-in.-diam sphere was fired at 6000 and 1 atm, providing a Reynolds number based on sphere diameter, projectile speed and ambient density and temperature of about 2×10^6.

At $X/D = 0$ (Fig. 1a) irregularities in the otherwise smooth fringe pattern near the wake centerline, show that the wake is turbulent and growing into the inviscid wake. At $X/D = 25$ (Fig. 1b) turbulent fluctuations begin to perturb the parallel inviscid-wake fringe pattern. At $X/D = 100$ (Fig. 1c) the turbulent wake begins to perturb the bottom edge of the inviscid wake. The fringe structure on the upper side of the wake being unperturbed relative to the lower side, points to the statistical description of the wake which an "instantaneous" picture captures. At $X/D = 200$ (Fig. 1d) an interaction between the turbulent wake and the inviscid flow is in evidence. At $X/D = 400$ (Fig. 1e) large scale fluctuations are observed along the edge of the inviscid wake. This irregularity gives rise to an intermittency of the wake turbulence, which would be observed, say, by an anemometer probe positioned at the edge of the wake. Large length scale disturbances having small density gradients are observed outside the wake. Finally, at $X/D = 1000$ (Fig. 1f), the wake width has grown to about 6 sphere diameters.

Sphere Wakes—Finite Fringe Interferograms

Three finite fringe holographic interferograms are shown in Fig. 2, namely, at 0, 50, and 200 X/D. In Fig. 2a, a maximum positive shift of about +4 fringes is observed in the compression region near the bow shock; the expansion about the sphere and the hot inviscid wake cause the fringe shift to become negative behind the projectile. A shift of about $+\frac{1}{2}$ fringe is encountered at the wake shock before fringe shift continues to take on larger negative values as the "hot" wake centerline is approached. Irregularities in fringe spacing on the centerline indicate that the wake is turbulent (however, this is more evident in Fig. 1a). In Fig. 2a, the inviscid wake is shown by the large rounded fringe contour.

Cone Wakes—Infinite Fringe Interferograms

Sharp-nosed, 12.5° half-angle, $\frac{3}{8}$-in.-base-diameter cones were fired at about 6300 fps and 1 atm. A sequence of cone wake pictures for $0 \leqq X/D \leqq 114$ is shown in Fig. 3, and the interesting properties of the wake are discussed below.

For $X/D = 0$ (Fig. 3a) the flowfield is similar to that around the sphere except that the inviscid wake for the cone is narrower and density gradients smaller than for the sphere. The edge of the inviscid wake can be observed as the symmetrical light fringe running parallel to and about one base diameter removed from the wake centerline starting at about $X/D = 10$.

The turbulent eddies are just about to break through the inviscid wake at $X/D = 70$ (Fig. 3b). At $X/D = 114$ (Fig. 3c) the

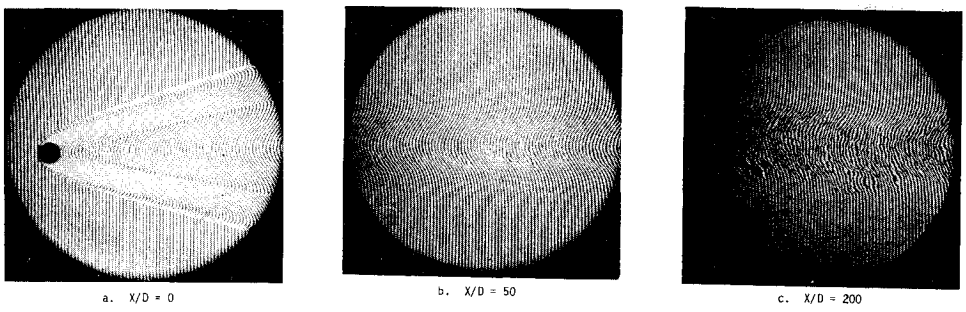

Fig. 2 Finite fringe holographic interferograms of wake of $\frac{1}{2}$-in. sphere fired at 6000 fps, 1 atm.

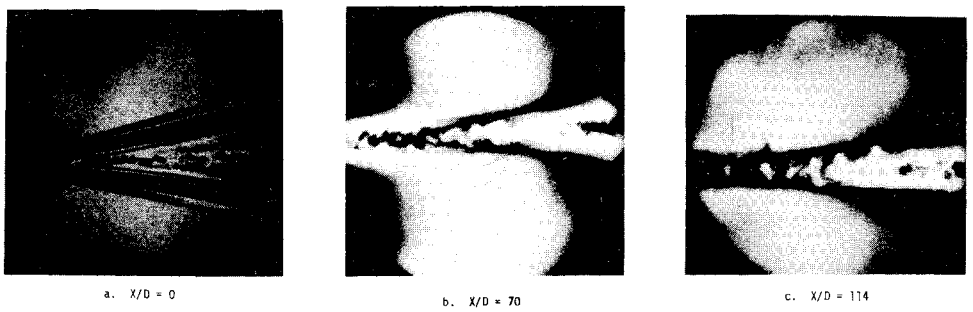

Fig. 3 Infinite fringe holographic interferograms of wake of 12.5° half-angle, $\frac{3}{8}$-in.-base-diam cone fired at 6300 fps, 1 atm.

viscous wake reaches the edge of the heated inviscid layer at this point and seems to literally explode over a distance of about 10 diam. Also interesting to note is the individual eddy which broke through the inviscid wake just prior to the point of complete breakthrough.

Turbulent Wake Density Fluctuation Measurements and Calculations

Data Reduction Technique

After some experimentation it was found that different axial locations had to be analyzed by different techniques. As one can see from the wake photographs, the low X/D turbulence data consist of fractional fringe variations about one mean fringe (low turbulent activity inside the viscous wake). On the other hand, the 200 and 400 X/D data (here breakthrough has occurred) show large-scale fluctuations across the whole wake.

The first method, which is used for the low X/D data, the microdensitometer method, uses the output of the microdensitometer directly. Such a trace, which is really the edge view of a plane passing through the interferogram, is referred to as a data length. By using the 3-D properties of holograms, data lengths can be taken from different angular views of the cone hologram. Close to the body, where the fringes are not parallel to the wake axis (the pressure field is changing) the mean fringe changes were eliminated by evaluating the fluctuations about the changing mean flow.

The method used for the large X/D data reduction is the contour map method. For this method radial surveys are taken at close intervals along the wake axis with the microdensitometer. From these surveys it is possible to reconstruct the interferograms by plotting full, half, and quarter fringes. The result is a contour map on which quarter fringe values are shown. It is now possible to pick a data length along the wake and obtain fringe values along this line by interpolating between the nearest plotted quarter fringe lines.

A representation of fringe value along a data length is thus obtained in a form suitable for use as input to standard statistical analysis programs. Correlation functions and power spectra can be computed. It is important that as long a data length as possible is chosen, approximately ten body diameters, in order to get a good low frequency resolution from the statistical analysis. Approximately 13 body diameters of data can be recorded with this holograph optics field of view. The data length must not be too long, however, in order to keep the mean properties of the wake sensibly constant. When the statistical analysis is performed, the largest separation of points used in calculating the autocorrelation is 20% of the data length. The five calculation samples which result if a 20% "maximum lag" is chosen are then averaged to give the final autocorrelation. If the largest scales contained in the data are more than about 20% of the data length, they will not be resolved in the analysis. Possible methods of extending data lengths will be discussed below.

Single-Beam Integrated Wake Calculations

Where calculations were made for both methods of data reduction, cited previously, very good agreement was reached. In Fig. 4 a plot of power spectral density in the wake at 400 X/D is shown. The data were taken along the same data length and show that indeed the two methods are equal. It was now possible to use the two methods interchangeably.

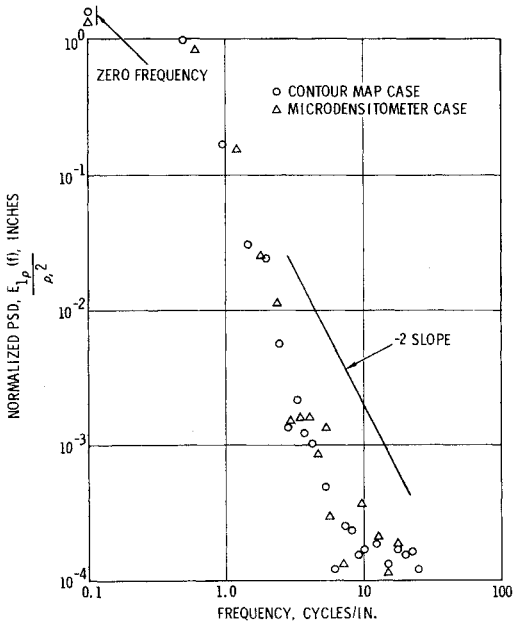

Fig. 4 Normalized power spectral density of sphere wakes at 400 X/D and $r/r_b = 1$.

One further improvement has been made to the technique in order to obtain a better description of the low frequency components in the wake. Since the over-all length of the data is restricted by the holocamera to 10–13 projectile diameters, and the statistical computation techniques have a largest possible data sample of 20% of the total data length, the longest fluctuation scale resolved is about 2.6 projectile diameters. There are scales larger than this contained in the wake, and they contribute significantly to the power. In order to define these low frequencies, it was decided to increase the data length by adding several single data lengths together.

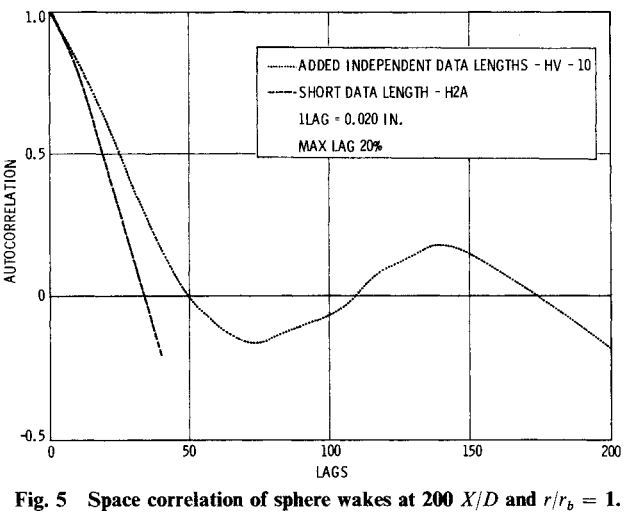

Fig. 5 Space correlation of sphere wakes at 200 X/D and $r/r_b = 1$.

In Fig. 5 space correlations are shown for representative calculations at 200 X/D. A short (or single) data length is compared here to a data length composed of four independent samples added together as just suggested. The four individual cases are made up from two data lengths taken from each of the two orthogonal wake holograms. All data lengths were taken at approximately one projectile radius from the wake axis. (The wake radius at this point is 1.6 projectile diameter.) It is seen from the result that the short length calculation gives only a representation of the small scales of the turbulence. The correlation function does go to zero but does not damp out and approach zero at long lags. For the long (added independent data) sample, damping and oscillation about zero for the correlation is observed, and much better representation of the large fluctuation scales, than was possible for the single data length case, is obtained. The smooth drop-off of the curves near zero lag shows a small noise level. This is confirmed when we inspect the power spectra for the same cases (Fig. 6). Here the averaged spectra for four short calculations are compared to the spectrum obtained when all four cases are added to form one long calculation sample. It is interesting to see that both of these curves, constructed from different kinds of averages, agree very well. As one might expect, the long data case gives a much better representation of the zero frequency (autocorrelation integral) value than does the short case. The slope of the long case is about -2 whereas the slope of the average of the individual cases is somewhat steeper. This seems to indicate that the short samples just do not constitute a long enough sample to permit satisfactory statistical analysis.

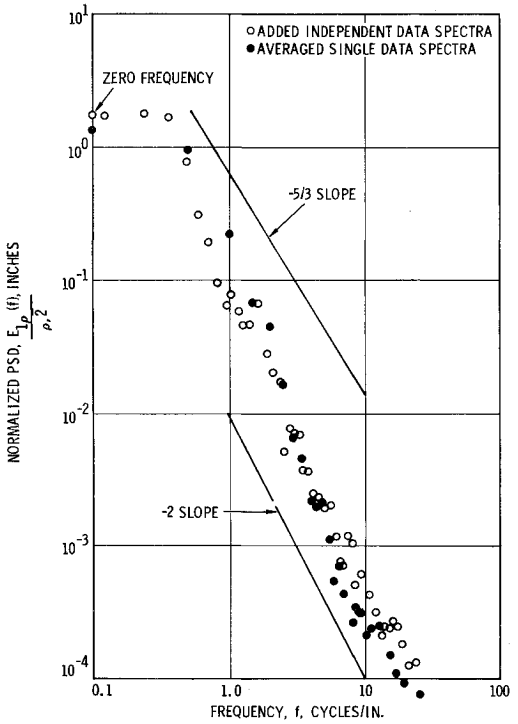

Fig. 6 Normalized power spectral density of sphere wakes at 200 X/D and $r/r_b = 1$.

Crossed-Beam Localized Wake Calculations

The concept of crossed-view localization of turbulent fluctuations depends on the fact that the main contribution to the cross correlation of fringe values read along crossed views is from the region of intersection of the views. This is true because outside the region of intersection, the turbulent fluctuations along a line of sight in each view are uncorrelated. The theory describing the application of cross viewing analysis of holographic interferograms of turbulent wakes to obtain local statistical properties of turbulence is given in Ref. 3. In order to obtain the cross views, orthogonal views of the wake were

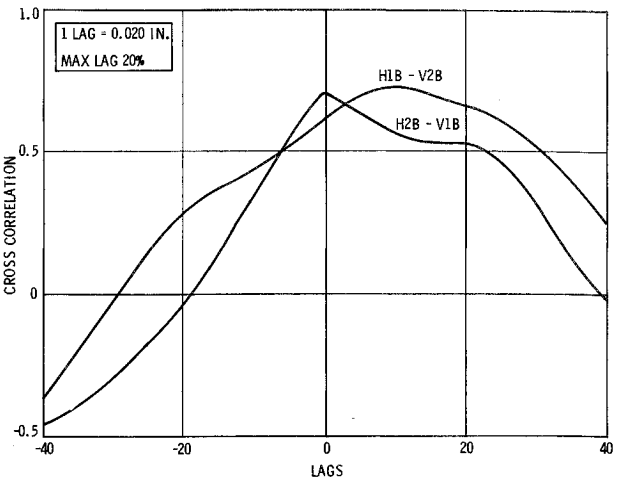

Fig. 7 Cross correlation of sphere wakes at 200 X/D and $r/r_b = 1$.

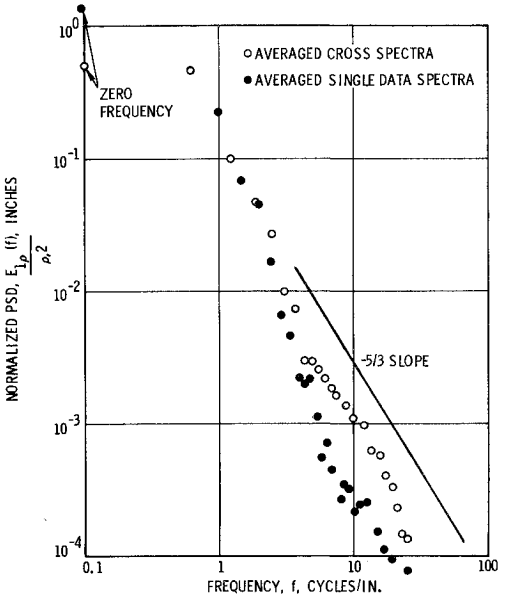

Fig. 8 Normalized power spectral density and cross spectra of sphere wakes at 200 X/D and $r/r_b = 1$.

taken simultaneously with the holocamera. The data used for the cross viewing analysis were then obtained in similar fashion as discussed above for the single views (the four data lengths used in this analysis were actually the same as used for the cross views), only in this case cross correlations and cross spectra were calculated. In Fig. 7 several cross correlations are shown at $X/D = 200$ and $r/r_b = 1$. The cross view data lie in a plane inclined at 45° to the horizontal vertical planes. The data are well correlated, signified by the large peak value near zero lag. The slight off zero peak of one of the curves may be due to an alignment error of the two cross views and is well within acceptable limits.

In Fig. 8 is shown four averaged cross spectra compared to the four averaged single-beam integrated power spectra. The difference between the curves points out the difference between integrated and localized fluctuation measurements. The two curves are coincident for low values of the frequency, but at high frequencies the localized spectra show higher power. The wake interferograms show a series of large fluctuations with small-scale fluctuations superimposed. Below a certain size of eddy, there will be a large enough number of these small wavelength fluctuations to provide a random variation in density across the wake width. Then as one integrates over these small random fluctuations through the wake, the net contribution will be very small, and on a PSD one can expect the curve to drop sharply at high frequencies. This trend is what is observed in Fig. 8. For the cross-view measurements, the fluctuations are considered locally at the line of intersection and the high frequencies are

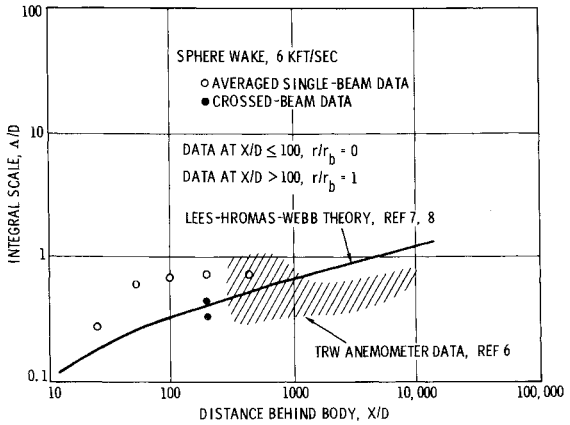

Fig. 9 Space correlation length of sphere wakes.

not averaged out but contribute to the power spectrum. In fact, it is observed that the slope of the localized (or cross) spectra is much closer to a $-\frac{5}{3}$ (Kolmogoroff) slope than the slope for the integrated data. At low frequencies the two spectra agree well with each other which is a reasonable behavior since there are not enough large fluctuations to form a random sample in the integrated case.

The slopes of the power spectra presented here are, in general, steeper than the Kolmogoroff $-\frac{5}{3}$ slope, less so for the localized values than for the single-beam integrated cases, and they do agree well wth the data by Fox.[6] A space correlation length scale Λ obtained from the autocorrelation integral[9]

$$\Lambda = \tfrac{1}{4}E_{1\rho}(0)/\rho'^2$$

was calculated for the data and compared with the anemometer data,[6] and estimates from the LHW theory (Fig. 9). The single-beam data lie close to, but somewhat above the theoretical estimates, and within the projected range of the anemometer data. The values for the length scale at most X/D locations (all except the 25 and 50 X/D cases) are averages over 2–10 cases. Included in the 200 and 400 X/D data are values from various radial positions in the wake, data from both orthogonal views of the wake, and data from the added independent data cases. At 100 X/D values from several radial positions in the wake were averaged. Shown also in Fig. 9 are two cases at 200 X/D which have been calculated using the crossed-beam localization technique. These data are in excellent agreement wth the LHW prediction. Better agreement with the LHW theory for these data as compared to the single-beam integrated data, supports the idea mentioned earlier that single-beam spectra may not accurately predict statistical properties. As more crossed-beam data are processed, this idea will be checked in detail.

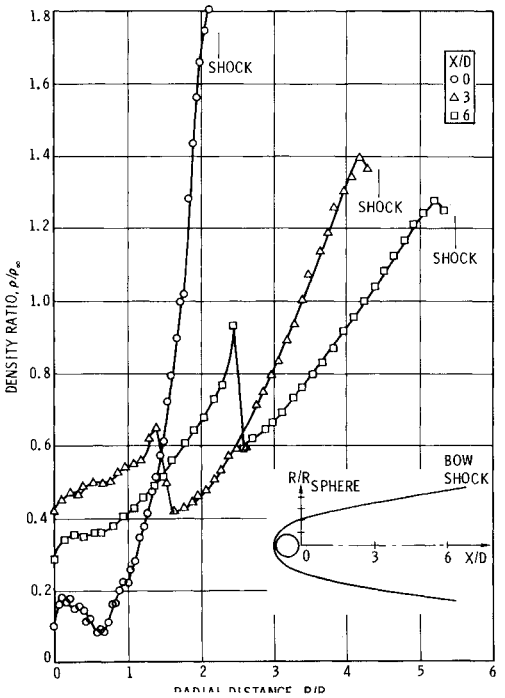

Fig. 10 Mean flow density profiles behind sphere fired at 6000 fps, 1 atm.

Only preliminary statistical data for cone wakes have been calculated. The integral scale, Λ/D, averaged from 5 data lengths between 30–70 X/D, is 0.18 which is above the LHW prediction by about 25%. Long data lengths were constructed by copying one hologram at three different angles and reading the data along the wake centerline. This technique is made possible because of the 3-D viewing properties of holograms.

Wake Mean Flow Measurements and Calculations

Mean Wake Density

Mean wake density was calculated at 0, 3, 6, 25, 50, 100, 200, 400, and 1000 X/D. At 0, 3 and 6 X/D where the pressure field had not recovered to p_∞, radial density profiles were calculated from the bow shock wave to the wake centerline as shown in Fig. 10. With the assumption of axial symmetry, the Abel inversion integral was used to obtain the density profiles.[1] Although no detailed flowfield calculations have yet been made at $M_\infty = 5.3$, nor experimental results available for purposes of comparison at low X/D, qualitatively the profile data appear to

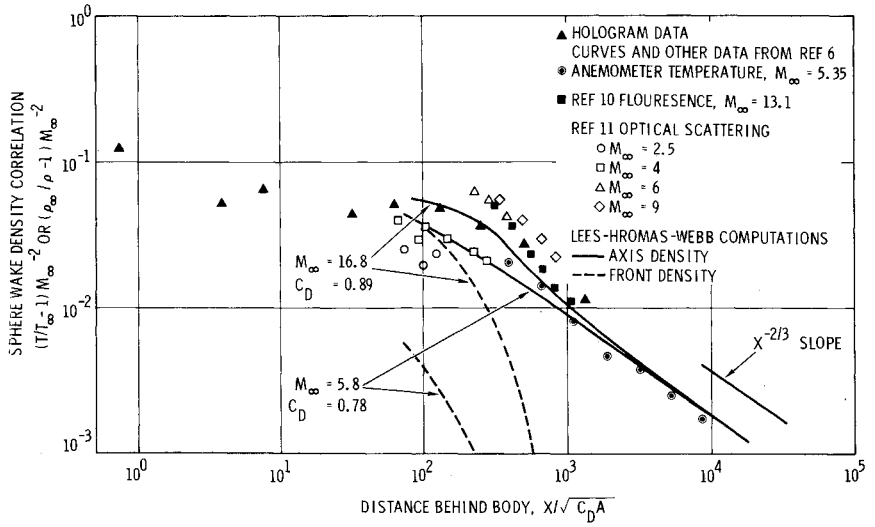

Fig. 11 Sphere wake density correlation.

be correct—compression at the bow shock, rapid expansion around the sphere, and either a slight over-expansion near the wake centerline (shown for the profile at $X/D = 0$) or compression by the wake shock (shown for the profiles at $X/D = 3$ and 6). The resolution of the data is quite good and proves that good mean flow data can be obtained from the use of pulsed laser holography in a large ballistic range.

For data at 25 X/D and beyond, the calculations were carried out between the edge of the inviscid wake and the wake centerline. Four radial profiles were calculated for each position at 25 X/D and beyond by using the Abel inversion integral. Then the individual density profiles were averaged to obtain a mean density profile. The standard deviation from the average ranged between 13–27% of the mean density. It was necessary to average the data because the centerline fringe pattern differed slightly for each profile because of wake turbulence. The error in density, believed to be less than about 10%, is less than the standard deviation caused by turbulent fluctuations.

The wake centerline density measurements are compared to Fox's anemometer measurements,[6] fluorescence,[10] and optical scattering[11] measurements, and the LHW theory for wakes in Fig. 11. Except for the hologram data which range from $\frac{1}{2} < X/D < 1000$, the curves and other data are from Fox.[6] The temperature parameter on the ordinate is suggested by the energy equation[6] with the condition of constant total enthalpy. The temperature and density parameters are equal under conditions of constant pressure and gas constant. The constant pressure assumption is probably valid for $X/(C_DA)^{1/2} > 80$. Thus, a convenient means of comparing temperature and density measurements is presented over a range of Mach number.

In the region of overlap the hologram yields lower ρ/ρ_∞ data [higher $(\rho_\infty/\rho - 1)$ data] which are no more than 12% less than the anemometer measurements. The agreement is within the spread of the turbulent density values calculated on the centerline from the holograms. The trend shown in Fig. 11 is consistent with the fact that the hologram density, calculated along the wake centerline, should be somewhat lower than the anemometer measurements made at least one sphere radius off the wake centerline.

The fluorescence measurements of ρ were made by electron beam excitation of nitrogen at pressures up to 7.6 mm Hg using a 2.7-in.-diam projectile.[10] These data lie above the LHW prediction at low $X/(C_DA)^{1/2}$. The optical scattering measurements of Ref. 11 are above both the hologram data and the prediction at $M_\infty = 6$ but show a strong dependence on M_∞, the trend projecting better agreement with the hologram data at $M_\infty = 5.3$. As mentioned earlier, for the region $0.5 < X/(C_DA)^{1/2} < 10^2$, no data from other sources exist for comparison purposes. The trend of the data appears correct; for example, the dip at $X/(C_DA)^{1/2} = 3.8$ is consistent with the strong recompression in density across the wake shock. The laser holograph technique appears to be especially useful to determine density field close to the body, say for $0 < X/(C_DA)^{1/2} < 1300$.

Because finite fringe interferograms have not been recorded of the cone wakes, only a few density profiles have been calculated between $0 \leqq X/D \leqq 13$ where fringe ambiguity could be resolved. Completed results will be included in a future publication.

Sphere Wake Velocity

In a region where the total enthalpy and the pressure are constant, and density measurement can be used to calculate the velocity using the definition of total enthalpy, $h_t = h + u^2/2$, and the assumption that the gas is thermally perfect $p = \rho RT$, and calorically perfect, $h = c_p T$.

The Lees-Hromas-Webb calculations[7,8] show that the constant pressure wake assumption is valid for $X/(C_DA)^{1/2} \leqq 80$ at $M_\infty = 22$. Calculations were not made at $M_\infty = 6$, but the wake pressure relaxes to ambient much faster for this condition. There are no "free flight" pressure measurements in this region to obtain confirmation of these results; however, the fringe pattern appears to confirm the results. The fringe pattern in the inviscid wake near the body remains nominally parallel and constant diameter. Were there a large change in wake pressure, the flowfield there would have responded by expanding or compressing the wake density field.

Fox[6] has shown for the same conditions, to within 20% accuracy of his measurements, the wake is adiabatic. A 20% error in total enthalpy yields approximately 10% error in velocity for the hypersonic wake.

The results are shown in Fig. 12 for the hologram data between $64 < X/(C_DA)^{1/2} < 1280$. Included also are electrostatic

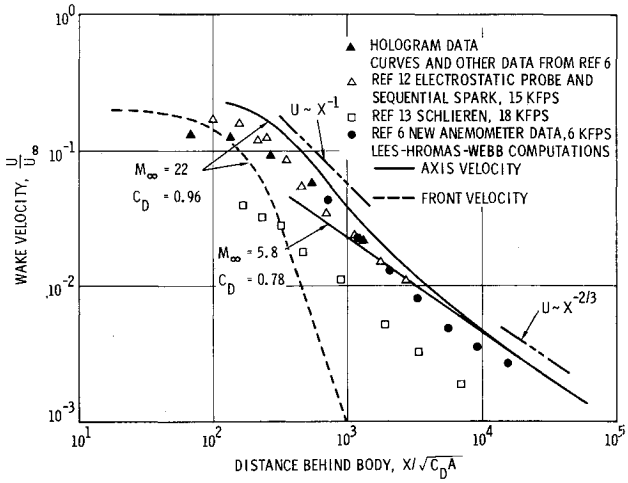

Fig. 12 Sphere wake velocity correlation.

probe and sequential spark data,[12] schlieren data,[13] the anemometer data,[6] and the LHW theory. Excellent agreement between the hologram and anemometer data is observed in the region of overlapping data. Very good agreement is also achieved there with the LHW prediction of axis velocity. Except for the schlieren data, agreement with the other data is good considering the trend of the data with M_∞.

Conclusions

1) A new method using pulsed laser holographic interferometry has been shown to be useful to investigate turbulent density fluctuations in projectile wakes from the base region to several hundred body diameters, where no other data are available. The axial sequence of interferograms shows the basic features of turbulent wake development as well as vividly contrasts the character of the "hot" sphere wake to the "cold" cone wake (see Section on Discussion of Wake Holographic Interferograms).

2) Integrated single beam spectra have been found to give a slope steeper than a $-\frac{5}{3}$ Kolmogoroff spectrum, but localized (crossed-beam) spectra approach a $-\frac{5}{3}$ slope. A plausible explanation, based on integrated vs localized properties, has been given to account for this data trend.

3) Wake correlation length scales were calculated from the autocorrelation integral over the range $0 < X/(C_DA)^{1/2} < 1300$. Single-beam values were found to lie somewhat above the Lees-Hromas-Webb (LHW) theory, but were in the range of the anemometer data at large $X/(C_DA)^{1/2}$. Two crossed-beam localized measurements of integral scale made at 200 X/D are in excellent agreement with the LHW theory. However, crossed-beam data at other axial locations in the wake need to be processed to confirm this trend.

4) The mean density and velocity on the wake axis are in good agreement with Fox's anemometer results[6] and the LHW theory. Density measurements are also shown near the body in a region where data had not previously existed.

References

[1] Witte, A. B. and Wuerker, R. F., "Laser Holographic Interferometry Study of High-Speed Flow Fields," AIAA Paper 69-347. Cincinnati, Ohio, 1969; also *AIAA Journal*, Vol. 8, No. 3, March 1970, pp. 581–583.

[2] Lien, H. and Eckerman, J., "Interferometry Analysis of Density Fluctuations in Hypersonic Turbulent Wakes," *AIAA Journal*, Vol. 4, No. 11, Nov. 1966, pp. 1988–1994.

[3] Witte, A. B., "Three Dimensional Flow Field Analysis by Holographic Photography and Interferometry," Rept. 12414-6003-R0-00, Nov. 1969, TRW Systems, Redondo Beach, Calif.

[4] Fox, J., "Statistical Analysis of a Turbulent Wake by Means of Laser Hologram Interferometry," Rept. 12414-6002-R0-00, June 1969, TRW Systems, Redondo Beach, Calif.

[5] Fisher, M. J. and Krause, F. R., "The Crossed-Beam Correlation Technique," *Journal of Fluid Mechanics*, Vol. 28, Pt. 4, 1967, pp. 705–717.

[6] Fox, J. and Rungaldier, H., "Anemometer Measurements of Velocity and Density in Projectile Wakes," *AIAA Journal*, Vol. 9, No. 2, Feb. 1971, pp. 270–276.

[7] Lees, L. and Hromas, L., "Turbulent Diffusion in the Wake of a Blunt Body at Hypersonic Speeds," Rept. 6110-005-MU000, July, 1971, TRW Space Technology Labs., Redondo Beach, Calif.; also *Journal of the Aerospace Sciences*, Vol. 29, 1962, pp. 976–993.

[8] Webb, W. H. and Hromas, L., "Turbulent Diffusion of a Reacting Wake," *AIAA Journal*, Vol. 3, No. 5, May 1965, pp. 826–837.

[9] Hinze, J. O., *Turbulence*, McGraw-Hill, New York, 1959.

[10] Tardiff, L. and Dionne, J. G. G., "Density Distribution in Turbulent and Laminar Wakes," *AIAA Journal*, Vol. 6, No. 10, Oct. 1968, pp. 2027–2029; also CARDE TN 1830/69, April 1969.

[11] Locke, E., "Point Measurements of Time-Averaged Turbulent Wake Density by Rayleigh Scattering," *AIAA Journal*, Vol. 5, No. 10, Oct. 1967, pp. 1888–1890.

[12] Heckman, D., Emond, A., and Sevigny, L., "Some Results of Electrostatic Probe Studies of Turbulent Hypersonic Wake Plasmas," AIAA Paper 68-689, Los Angeles, Calif., 1968.

[13] Herrman, J., Slattery, R. E., and Clay, W. G., "Measured Properties of the Wakes of Hypersonic Cones," AIAA Paper 68-687, Los Angeles, Calif., 1968.